UNIVERSITÀ DEGLI STUDI DI MILANO

FACOLTÀ DI SCIENZE E TECNOLOGIE

CORSO DI LAUREA IN FISICA

TESI DI LAUREA TRIENNALE

A machine learning approach to the electrons and photon classification with the ATLAS detector at the LHC

Autore:
Pietro Daniele

Matricola:
906962

Codice P.A.C.S.:
07.05.-t

Relatore:
Prof. Leonardo Carlo Carminati

Corelatori:
Dott. Ruggero Turra
Dott. Davive Mungo

Anno accademico 2019-2020

Contents

Chapter 1

LHC and ATLAS

1.1 The LHC

The CERN Large Hadron Collider is a two-ring, superconducting accelerator and collider installed in the long LEP tunnel (27 km)[1] and it provides pp collisions and heavy-ion (e.g. Pb-Pb) collision.
Inside the accelerator, two high-energy particle beams travel at close to the speed of light before they are made to collide. The beams travel in opposite directions in separate beam pipes (two tubes kept at ultrahigh vacuum). They are guided around the accelerator ring by a strong magnetic field maintained by superconducting electromagnets[2]

1.1.1 Lattice Layout

The basic layout of the LHC follows the LEP tunnel geometry. The LHC has eight arcs and straight sections. Each straight section is approximately 528 m long and can serve as an experimental or utility insertion. The two high luminosity experimental insertions are located at diametrically opposite straight sections: the ATLAS experiment is located at point I and the CMS experiment at point 5.
Two more experimental insertions are located at point 2 and point 8 which also contain the injection systems for Beam J and Beam 2, respectively. The injection kick occurs in the vertical plane with the two beams arriving at the LHC from below the LHC reference plane. The beams only cross from one magnet bore to the other at these four locations.
The remaining four straight sections do not have beam crossings. Insertion 3 and 7 each contain two collimation systems. Insertion 4 contains two RF systems: one independent system for each LHC beam. The straight section at point 6 contains the beam dump insertion where the two beams are vertically extracted from the machine using a combination of horizontally deflecting fast-pulsed ('kicker') magnets and vertically-deflecting double steel septum magnets. Each beam features an independent abort system. [1]
The protons travel inside along th LHC ring in opposite direction. The LHC beams are controlled by superconducting magnets, which have a working temperature of 1.9 K. There are two kinds of superconducting magnets:
- the superconducting dipole magnets, which thanks to a 8.33 T magnetic field drive protons along the ring (circular orbit);
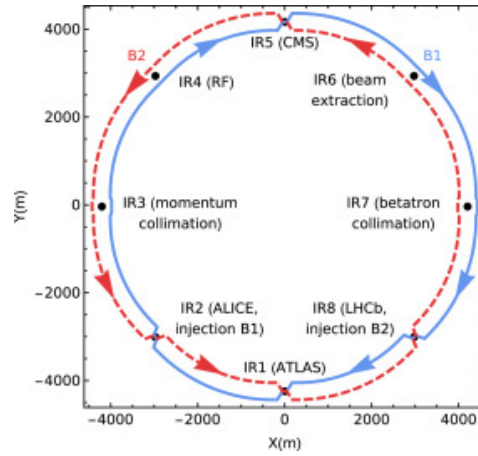- superconducting quadrupole magnets, which keep the beams focused.
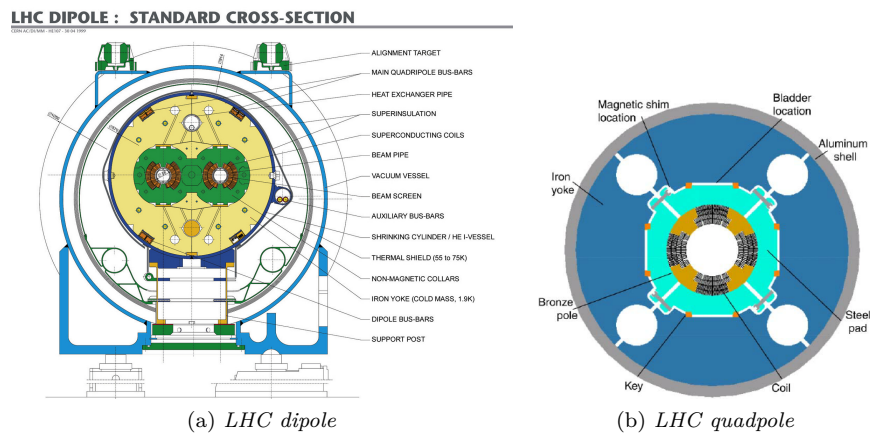
Figure 1.1: LHC structure

(a) *LHC dipole*

(b) *LHC quadpole*

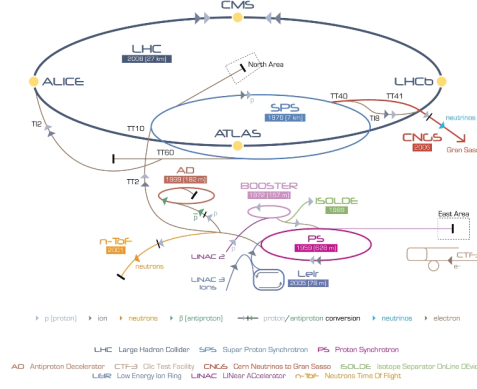Figure 1.2: LHC's superconducting magnets

Figure 1.3: LHC and CERN's complex accelerator

1.1.2 The CERN accelerator complex

Before being insert into LHC ring, particle beam is accelereted by the CERN accelerator complex. It is a succession of machins with increasingly higher energies. Each machine injects the beam into the next one, which takes over to bring the beam to an even higher energy, and so on. In the LHC—the last element of this chain—each particle beam is accelerated up to the record energy of 6.5 TeV. Specifically, in LHC protons are obtained by stripping electrons from hydrogen atoms, which are taken from a bottle containing hydrogen. Then protons are injected into the PS Booster (PSB) at an energy of 50 MeV from Linac2. The booster accelerates them to 1.4 GeV. The beam is then fed to the Proton Synchrotron (PS) where it is accelerated to 25 GeV. Protons are then sent to the Super Proton Synchrotron (SPS) where they are accelerated to 450 GeV. They are finally transferred to the LHC (both in a clockwise and an anticlockwise direction) where they are accelerated for 20 minutes to 6.5 TeV. Beams circulate for many hours inside the LHC beam pipes under normal operating conditions.
In addition to accelerating protons, the accelerator complex can also accelerate lead ions. [3]

1.1.3 Proton-proton collisions

The numer of events per second generated in the LHC collisions is given by:

$$N_{event} = L\sigma_{event}$$

where σ_{event} is the cross section for the event under study and L the machine luminosity. L depends only on the beam parameters and can be written for a Gaussian beam distribution as:

$$L = \frac{N_b^2 n_b f_{rev} \gamma_r}{4\pi \epsilon_n \beta^*} F$$

[1] where N_b is the number of particles per bunch, n_b the number of bunches per beam, f_{rev} the revolution frequency, γ_r the relativistic gamma factor, ϵ_n the normalized transverse beam emittance, β^* the beta function at the collision point and F the geometric luminosity reduction factor due to the crossing angle at the IP.

The total inelastic proton-proton cross-section is about 80 mb at $\sqrt{s} = 14$ TeV. [2] Therefore, the event rate R, defined as the number of events produced per second by the pp interactions, is

expected to be:

$$R = \sigma L = 80mb \times 10^{34} cm^{-2} s^{-1} \simeq 10^9 s^{-1}$$

There are towo types of pp collisions:

- Soft collisions: they are the most of the collisions and they are large-distance collisions between the two incoming protons. They are called "soft" because the momentum transfer of the interaction is small. Due to this feature, particle scattering at large angle is suppressed and so, after collisions, particles have a large longitudinal momentum, but small transverse momentum ($< p_T > \simeq 500 Mev$) relative to the beam line. The final states arising from such interactions are called minimum bias events. They are not interesting.

- Hard collisions: monochromatic proton beams can be seen as beams of partons (quarks and gluons) with a wide band of energy. Occasionally, head-on collisions occur between two partons of the incoming protons. These are interactions at small distances, and therefore are characterised by large momentum transfers ("hard scattering"). In this case, particles in the final state can be produced at large angles with respect to the beam line (high p_T) and massive particles can be created. These are the interesting physics events. They are, however, rare compared to the soft interactions.

  In the hard-scattering interactions of quarks and gluons at a hadron collider, the effective centre-of- mass energy of the interaction ($\sqrt{\hat{s}}$) is, u, smaller than the centre-of-mass energy of the machine ($\sqrt{s}$) and is given by:

$$\sqrt{\hat{s}} = \sqrt{x_a x_b s}$$

  where x_a and x_b are the fractions of the proton momentum carried by the two colliding partons. If $x_a \simeq x_b$, then the above relation becomes

$$\sqrt{\hat{s}} \simeq x\sqrt{s}$$

  . Therefore, in order to produce a particle of mass 100 GeV, two quarks (or gluons) which carry only 1% of the proton momentum are needed ($x \sim 0.01$), whereas a particle of mass 5 TeV can only be produced if two partons with $x \sim 0.35$ interact. The momentum distributions of quarks and gluons inside the proton are called parton distribution functions. [2]

1.2 ATLAS

[4]ATLAS is one of two general-purpose detectors at the Large Hadron Collider (LHC). It investigates a wide range of physics, from the search for the Higgs boson to extra dimensions and particles that could make up dark matter. Although it has the same scientific goals as the CMS experiment, it uses different technical solutions and a different magnet-system design.

Beams of particles from the LHC collide at the centre of the ATLAS detector making collision debris in the form of new particles, which fly out from the collision point in all directions. Six different detecting subsystems arranged in layers around the collision point record the paths, momentum, and energy of the particles, allowing them to be individually identified. A huge magnet system bends the paths of charged particles so that their momenta can be measured.

The interactions in the ATLAS detectors create an enormous flow of data. To digest the data, ATLAS uses an advanced "trigger" system to tell the detector which events to record and which to ignore. Complex data-acquisition and computing systems are then used to analyse the collision events recorded. At 46 m long, 25 m high and 25 m wide, the 7000-tonne ATLAS detector is the largest volume particle detector ever constructed.
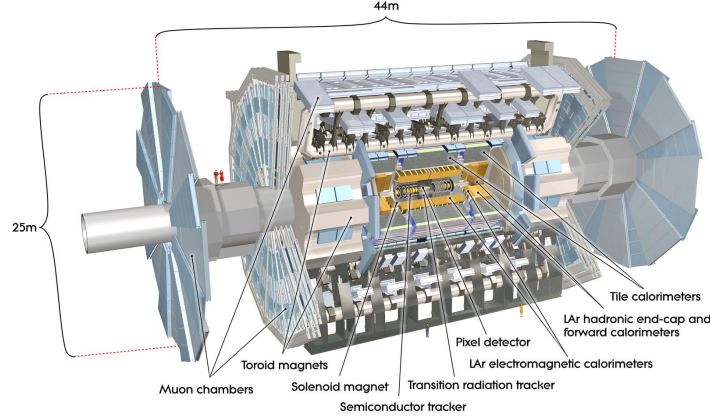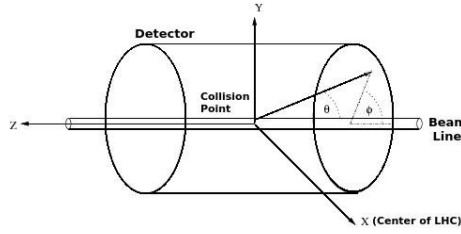
Figure 1.4: ATLAS structure

Figure 1.5: ATLAS coordinate system

1.2.1 Coordinate system

[5]The origin of the coordinate system is set in the nominal point of interation. The beam direction defines the z-axis and the x-y plane is transverse to the beam direction. X-axis points from the interaction point to the centre of the LHC ring and Y-axis points upwards. The side-A of the detector is defined as that with positive z and side-C is that with negative z.

Polar coordinate are also used: azimuthal angle ϕ is measured as usual around the beam axis, and the polar angle θ is the angle from the beam axis. Using θ, pseudo rapidity is defined as $\eta = -\ln \tan \frac{\theta}{2}$.

The transverse momentum p_T, the transverse energy E_T, and the missing transverse energy E_T^{miss} are defined in the x-y plane unless stated otherwise. The distance ΔR in the pseudo rapidity-azimuthal angle space is defined as $\Delta R = \sqrt{\Delta\eta^2 + \Delta\phi^2}$.

1.2.2 Magnet system

[5]ATLAS features a unique hybrid system of four large superconducting magnets. This magneticsystem is 22 m in diameter and 26 m in length, with a stored energy of 1.6 GJ.
The ATLAS magnet system consists of:

- a solenoid, which is aligned on the beam axis and provides a 2 T axial magnetic field for the inner detector, while minimising the radiative thickness in front of thebarrel electromagnetic calorimeter;
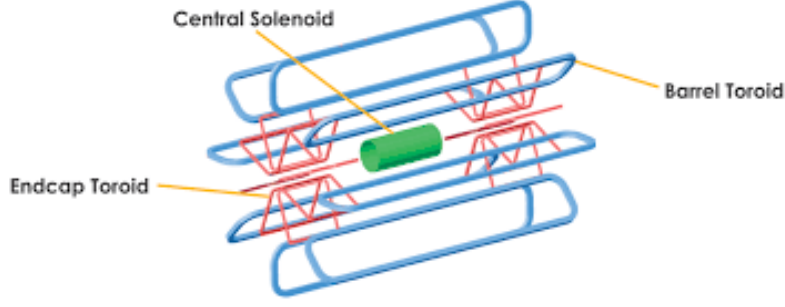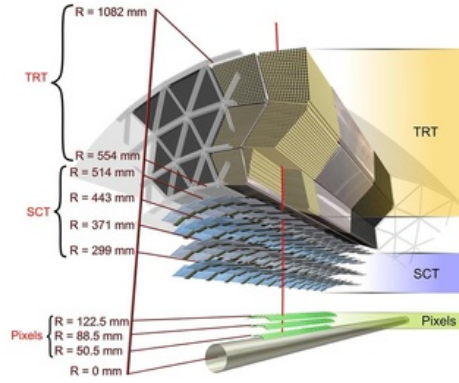
Figure 1.6: ATLAS magnet system

Figure 1.7: ATLAS Inner Detector structure

- a barrel toroid and two end-cap toroids, which produce atoroidal magnetic field of approximately 0.5 T and 1 T for the muon detectors in the centraland end-cap regions, respectively.

1.2.3 Inner detector

The ATLAS Inner Detector (ID) is the inner-most ATLAS layer and it is immersed in a 2 T solenoidal field. It is designed to provide hermetic and robust pattern recognition, excellent momentum resolution and both primary and secondary vertex measurements forcharged tracks, with a lower limit in p_t (nominally 0.5 GeV, but as low as 0.1 GeV) and within the pseudorapidity range $|\eta| < 2.5$. It also provides electron identification over $|\eta| < 2.0$ and a wide range of en-ergies (between 0.5 GeV and 150 GeV). [5]

ID is composed by three independent but complementary sub-detectors:

- Pixel Detector: [6] it is the inner-most part of the ATLAS tracking system. It consists of 4 layers of barrel pixel detector and two end caps of three pixel disks each. The innermost pixel layer is a high-resolution pixel detector, called Insertable B-Layer (IBL). The Pixel Detector sits inside the 2T solenoidal magnetic field and contributes to the charged particle tracking of the ATLAS Inner Detector in the pseudo rapidity range of $|\eta| < 2.5$. Due to its high spatial resolution and 3-dimensional space-point measurement the Pixel Detector has

a key-role in reconstruction of charged particle tracks. The 4-Layer Pixel Detector will be crucial in the reconstruction of primary and secondary vertices which is essential for the detection of long-lived particles.

- Semiconductor Tracker (SCT): [7] it consists of 61 m^2 of active silicon-strip detector modules and it is immersed in a 2 T solenoidal magnetic field. The SCT covers the radial region from 30 to 52 cm, with hermetic azimuthal coverage out to $|\eta| = 2.5$. Four cylindrical layers in the central region form the "barrel" detector, and nine annulardisks on each end of the barrel form the "endcaps". The layout has been designed so that energetic charged particles will pass through at least four layers everywhere in the acceptance region.

- Transition Radiation Tracker (TRT): [8] it is the outmost f the three tracking subsystems of the ATLAS Inner Detector. TRT s a straw-tube tracker and it consists of drift tubes with a diameter of 4 mm that are made from wound Kapton and reinforced with thin carbon fibres.
  When a charged particle traverses the TRT, it ionises the gasinside the straws. The resulting free electrons drift towards thewire, where they are amplified and read out.
  The spaces between the straws are filled with polymer fibres(barrel) and foils (endcaps) to create transition radiation, whichmay be emitted by highly relativistic charged particles as theytraverse a material boundary. This effect depends on the rel-ativistic factor $\gamma = E/m$ and is strongest for electrons. This design makes the TRT complementary to the silicon-based tracking devices: the intrinsic single-point resolution of 120 μm is larger than that of the silicon trackers, but this is compensated by the large number of hits per track (typically morethan 30) and the long lever arm. Furthermore, the high sam-pling frequency of the wire signals enables the TRT to providetiming information on the nanosecond level. RIFAI MEGLIOOOOOOOO OOOOOOOOOOOO OOOOOOOOOOOO OOOOOOOOOOOO OOOO
  OO OOOOOOOOOOOOOOOO
  OOO OOOOOOOOOO O OOOOOOOOOOOOOOOO
  OOOOOOOO

1.2.4 Calorimetry system

Calorimeters measure the energy a particle loses as it passes through the detector, so the energy of all charged and neu- tral particles. It is usually designed to stop entire or "absorb" most of the particles coming from a collision, forcing them to deposit all of their energy within the detector. Calorimeters typically consist of layers of "passive" or "absorbing" high-density material interleaved with layers of an "active" medium such as solid lead-glass or liquid argon. Calorimeters can stop most known particles except muons and neutrinos.

The components of the ATLAS calorimetry system are: [9]

- electromagnetic calorimetry: The main part of ATLAS EM calorimeter is alead–liquid argon (LAr) sampling detector with accordion-shaped electrodes and lead absorber plates over its full coverage. The calorimeter isdivided into a Barrel part and two End-Caps (seeTable 1). Each End-Cap is divided into two coaxial wheels: an outer wheel and an inner wheelcovering, respectively, 1:375ojZjo2:5 and 2:5o. The absorber lead thickness is constantover large areas. The argon gap thickness isconstant in the Barrel but changing with theradius in the End-Cap.There are three longitudinal samplings forjZjo2:5 and two for 2:5ojZjo3:2:. n the rangejZjo1:8;the calorimeter is precededby a presampler (see Table 1) to recover the energylost in the upstream material (cryostat, super-conducting coil, inner

detector, etc.). The activedepth of the presampler is 11 mm of liquid argonin the Barrel and 4 mm in the End-Cap.

- hadronic calorimeters: In the range$jZjo1:6$;the ATLAS hadroniccalorimeter is an iron-scintillating tiles calorimeter.For rapidity larger than 1.6, the hadronic calori-meter is an LAr calorimeter. The Hadronic Tile calorimeter is located behindthe solenoid coil and the EM calorimeter. It is asampling calorimeter using iron as absorbermaterial and scintillating tiles as active material. The Hadronic End-Cap calorimeter (HEC) is anLAr sampling calorimeter which provides hadro-nic coverage for $1:5ojZjo3:2$

- forward calorimeters (FCal): In the forward region ($3:1ojZjo4:9$), the EMcalorimetry is done by another type of LArcalorimeter. The Forward Calorimeter (FCAL)consists of copper rods parallel to the beam axisinside an outer tube with 250mm liquid argon gapin between

1.2.5 Muon spectrometer

The muon spectrometer forms the outer part of the ATLAS detector and is designed to de-tectcharged particles exiting the barrel and end-cap calorimeters and to measure their momentum inthe pseudorapidity range$|\eta| < 2.7$. It is also designed to trigger on these particles in the region$|\eta| < 2.4$.

Chapter 2

Electron and photon reconstruction

Events with electrons and photons in the final state are important signatures for many physics analyses envisagedat the LHC. Their reconstruction mainly exploits data coming from the electromagnetic calorimeter (clusters) and the Inner Detector (ID) systems (tracks) [10]:

- an electron is defined as an object consisting of a cluster built from energy deposits in the calorimeter (supercluster) and a matched track (or tracks);

- a converted photon is a cluster matched to a conversion vertex (or vertices), and an unconverted photon is a cluster matched to neither an electron track nor a conversion vertex. About 20% of photons at low $|\eta|$ convert in the ID, and up to about 65% convert at $|\eta| \simeq 2.3$.

The reconstruction with $|\eta| < 2.5$ is based on an algorithm. It first prepares the tracks and clusters it will use. It selects clusters of energy deposits measured in topologically connected EM and hadronic calorimeter cells, denoted topo-clusters. These clusters are matched to ID tracks, which are re-fitted accounting for bremsstrahlung. The algorithm also builds conversion vertices and matches them to the selected topo-clusters. The electron and photon supercluster-building steps then run separately using the matched clusters as input. After applying initial position corrections and energy calibrations to the resulting superclusters, the supercluster-building algorithm matches tracks to the electron superclusters and conversion vertices to the photon superclusters. The electron and photon objects to be used for analyses are then built, their energies are calibrated, and discriminating variables used to separate electrons or photons from background are added.

2.1 The topo-cluster reconstruction

The topo-cluster reconstruction algorithm begins by forming proto-clusters in the EM and hadronic calorimeters using a set of noise thresholds in which the cell initiating the cluster is EM required to have significance $|\zeta_{cell}^{EM}| \geq 4$ where

$$\zeta_{cell}^{EM} = \frac{E_{cell}^{EM}}{\sigma_{cell}^{EM}}$$

E_{cell}^{EM} is the energy cell at the EM scale and σ_{cell}^{EM} is the expected cell noise, which includes the known electronic noise and an estimate of the pile-up noise corresponding to the average instantaneous luminosity expected for Run 2. In order to suppres the formation of noise cluster, in this initial stage, cells from the presampler and the first LAr EM calorimeter layer are excluded from initiating proto-clusters. An important role is played by the neighbouring cells. If they have a significance $|\zeta_{cell}^{EM}| \geq 2$, these cells are collected by proto-cluster. Each neighbour cell passing the threshold of $|\zeta_{cell}^{EM}| \geq 2$ becomes a seed cell in the next iteration, collecting each of its neighbours in the proto-cluster. If two proto-clusters EM contain the same cell with $|\zeta_{cell}^{EM}| \geq 2$ above the noise threshold, these proto-clusters are merged. A crown of nearest-neighbour cells is added to the cluster independently on their energy ($|\zeta_{cell}^{EM}| \geq 0$). This set of thresholds is commonly known as '4-2-0' topo-cluster reconstruction.

Energy becomes an important feature when a cell has $|E_{cell}^{EM}| > 500$ MeV. A cell with this energy, at least four neighbours, and when none of the neighbours has a larger signal, is a local maximum. Proto-clusters with two or more local maxima are split into separate clusters.

2.2 Track reconstruction

Track finding is one of the most challenging tasks in reconstructing events from proton-proton collisions recorded by the ATLAS detector. The process consists in finding a track in the ID which can be matched to the energy clusters. The ID track reconstruction consists of several sequences with different strategies and the main sequence is referred to as inside-out track finding: [14]

- **Space point formation**: the initial step of the ID reconstruction consists of the cluster and drift circle creation and the transformation of clusters in the silicon detectors into 3D space points. Clusters are formed by finding connected cells in the pixel and strip detectors. [13]From these clusters, three-dimensional measurements referred to as space-points are created. In the pixel detector, each cluster equates to one space-point, while in the SCT, clusters from both stereo views of a strip layer must be combined to obtain a three-dimensional measurement.

- **Space point seeded track finding**: track seeds are formed from sets of three space-points in the silicon-detector layers. [14] Seeds can be built from space points in the pixel detector only (referred to as PPP seeds), the strip detector only (SSS) or any mixed setup (PSS,PPS). To reduce the number of potential seeds, initial cuts are applied and dedicated care is taken not to extensively use space points in multiple seeds. Seeds that pass the initial requirements are then input to a track finding algorithm that uses a combinatorial Kalman filter technique and aims to complete the track candidates within the silicon detector.

- **Ambiguity solving**: track candidates are then further processed in an ambiguity solving module that aims to eliminate track candidates from random hit combinations (often referred to as "fakes") or track duplicates, which can be identified by measurements that are shared with other track candidates. The ambiguity solving relies on a scoring function applying positive scores for unique measurements and good fit quality, while penalising missing measurements where they would be expected (also called holes) or shared measurements with other track candidates.

- **TRT extension**: tracks that successfully pass the ambiguity solving stage and are within the coverage of the TRT detector are then extended into the TRT and completed for measurements in the outermost tracking detector. A successful TRT extension increases the momentum resolution significantly by exploiting the longer lever arm for field integration.

2.3 Track-cluster matching and photon conversion reconstruction

2.4 Supercluster reconstruction

The reconstruction of electron and photon superclusters proceeds independently, each in two stages [11]:

1. in the first stage, EM topo-clusters are tested for use as seed cluster candidates, which form the basis of superclusters;

2. in the second stage, EM topo-clusters near the seed candidates are identified as satellite cluster candidates, which may emerge from bremsstrahlung radiation or topo-cluster splitting.

Superclusters are built through various sets:

- the initial list of EM topo-clusters is sorted according to descending E_T , calculated using the EM energy.

- the clusters are tested one by one in the sort order for use as seed clusters. There are two seed's kind:

    i. electron supercluster seed: a cluster with a minimum E_T of 1 GeV and matched to a track with at least four hits in the silicon tracking detectors.

    ii. photon supercluster seed: a cluster with E_T greater than 1.5 GeV with no requirement made on any track or conversion vertex matching.

  A cluster cannot be used as a seed cluster if it has already been added as a satellitecluster to another seed cluster.

- if a cluster meets the characteristics of the previous point, the algorithm attempts to find satellite clusters, using the process summarized in figure 2.1. For both electrons and photons, a cluster is considered a satellite if it falls within a window of $\Delta\eta \times \Delta\varphi = 0.075 \times 0.125$ around the seed cluster barycentre, as these cases tend to represent secondary EM showers originating from the same initial electron or photon. This window is a larger $\Delta\eta \times \Delta\varphi = 0.125 \times 0.300$
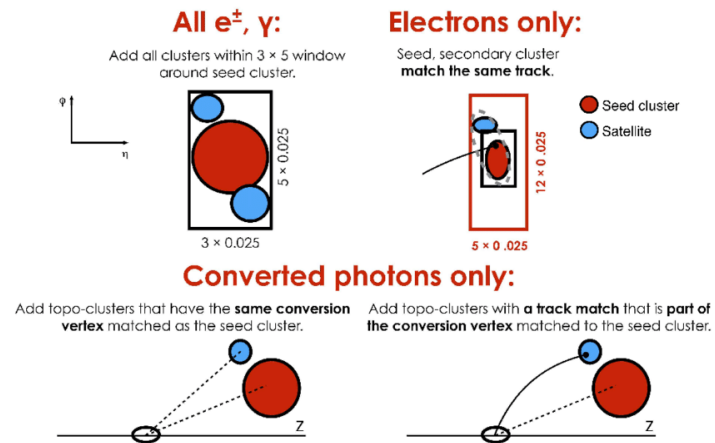
Figure 2.1: Diagram of the superclustering algorithm for electrons and photons. Seed clusters are shown in red, satellite clusters in blue.

Bibliography

[1] European organization for nuclear research, *LHC design report*, CERN libraries, Geneva (2004). `http://cds.cern.ch/record/782076/files/`

[2] F. Gianotti, *Collider physics: LHC*, EP Division, CERN, Geneva, Switzerland. `https://cds.cern.ch/record/458489/files/p219.pdf`

[3] `https://cds.cern.ch/record/2255762/files/CERN-Brochure-2017-002-Eng.pdf`

[4] `https://home.cern/science/experiments/atlas`

[5] The ATLAS Collaboration et al 2008 JINST3 S08003 `https://iopscience.iop.org/article/10.1088/1748-0221/3/08/S08003/pdf`

[6] H. Pernegger, *The Pixel Detector of the ATLAS Experiment for LHC Run-2*, ATL-INDET-PROC-2015-001. `https://cds.cern.ch/record/1985432/files/ATL-INDET-PROC-2015-001.pdf`

[7] J.R. Pater *The ATLAS SemiConductor Tracker operation and performance*, 2012 JINST7 C04001. `https://iopscience.iop.org/article/10.1088/1748-0221/7/04/C04001/pdf`

[8] Adrian Vogel *ATLAS Transition Radiation Tracker (TRT): Straw Tube Gaseous Detectors at High Rates*, CERN, Geneva, ATL-INDET-PROC-2013-005, Apr 2013, ATL-INDET-PROC-2013-005. `https://cds.cern.ch/record/1537991`

[9] `http://ific.uv.es/~cabrera/teaching/atlas_i.pdf`

[10] Wu Xin, Clark Allan and Campanelli Mario *Electron and photon identification in ATLAS*, Springer Berlin Heidelberg, Berlin, Heidelberg, 2006 `https://link.springer.com/chapter/10.1007/978-3-540-32841-4_21`

[11] *Electron and photon performance measurements with the ATLAS detector using the 2015-2017 LHC proton-proton collision data* `https://iopscience.iop.org/article/10.1088/1748-0221/14/12/P12006`

[12] *A neural network clustering algorithm for the ATLAS silicon pixel detector*, The ATLAS collaboration `https://doi.org/10.1088%2F1748-0221%2F9%2F09%2Fp09009`

[13] `https://link.springer.com/content/pdf/10.1140/epjc/s10052-019-7140-6.pdf`in

[14] *Optimisation of the ATLAS Track Reconstruction Software for Run-2*, Andreas Salzburger, CERN, Switzerland, `http://iopscience.iop.org/1742-6596/664/7/072042`